

ARTICLE

Open Access

Combinatorial control of *Spo11* alternative splicing by modulation of RNA polymerase II dynamics and splicing factor recruitment during meiosis

Eleonora Cesari^{1,2}, Maria Loiarro², Chiara Naro^{1,2}, Marco Pieraccioli², Donatella Farini^{2,3}, Livia Pellegrini^{2,3}, Vittoria Pagliarini^{1,2}, Pamela Bielli^{2,3} and Claudio Sette^{1,2} 

Abstract

Homologous recombination and chromosome segregation in meiosis rely on the timely expression of two splice variants of the endonuclease SPO11, named α and β , which respectively skip or include exon 2. However, in spite of its physiological importance, the mechanism underlying *Spo11* alternative splicing in meiosis is still unknown. By screening the activity of factors that are predicted to bind the alternatively spliced region of *Spo11*, we identified hnRNPH as a key regulator of SPO11 α splicing in mouse spermatocytes. Although hnRNPH was not upregulated in meiosis concomitantly with the switch in splicing, its recruitment to *Spo11* pre-mRNA was favored by selective modulation of RNA polymerase II (RNAPII) phosphorylation and processivity in proximity of exon 2. The hnRNPH binding sites were localized near those of splicing factors that promote SPO11 β splicing, suggesting that hnRNPH favors exon 2 skipping by competing out positive regulators. Indeed, hnRNPH binds proximal to a consensus motif for Sam68, a positive regulator of SPO11 β splicing in vitro and in vivo, and it interferes with Sam68 binding to the *Spo11* pre-mRNA. Thus, our work reveals that modulation of RNAPII dynamics in concert with hnRNPH recruitment exerts a combinatorial control of the timely regulated *Spo11* splicing during meiosis.

Introduction

Alternative splicing (AS) of pre-mRNAs is a powerful combinatorial mechanism that allows production of protein isoforms with different functions from each gene^{1,2}. AS modularity allows expansion of the coding potential of the genome and promotes plasticity in its utilization¹. Splicing reactions are orchestrated by a ribonucleoprotein complex called “spliceosome”, which recognizes exon–intron junctions, excises introns and ligates exons³. The lack of stringent consensus sequences at splice junctions in higher eukaryotes allows flexibility in their recognition. Numerous RNA-binding proteins (RBPs) act

as splicing factors by interacting with the spliceosome, and reinforce or weaken recognition of exon–intron junctions. The interplay between these antagonistic splicing factors determines the choice of regulated exons by the spliceosome and causes heterogeneity in pre-mRNA processing^{1,3,4}. In addition, AS is modulated by the rate of transcription and by epigenetic marks that decorate exons subject to regulation^{5,6}. As a consequence, changes in the expression and/or in the activity of any of the factors contributing to these processes can selectively influence AS regulation. In particular, the elongation rate of the RNA polymerase II (RNAPII) is a key factor in co-transcriptional selection of regulated exons. A fast elongation rate makes more splice sites concomitantly available within a pre-mRNA, allowing competition between them and generally favoring stronger splice sites, whereas a slow rate of elongation promotes inclusion of weak exons^{5,7}. However, genome-wide analyses indicated that

Correspondence: Claudio Sette (claudio.sette@unicatt.it)

¹Department of Neuroscience, Section of Human Anatomy, Catholic University of the Sacred Heart, 00168 Rome, Italy

²Laboratory of Neuroembryology, IRCCS Fondazione Santa Lucia, 00143 Rome, Italy

Full list of author information is available at the end of the article

Edited by G. Melino

© The Author(s) 2020



Open Access This article is licensed under a Creative Commons Attribution 4.0 International License, which permits use, sharing, adaptation, distribution and reproduction in any medium or format, as long as you give appropriate credit to the original author(s) and the source, provide a link to the Creative Commons license, and indicate if changes were made. The images or other third party material in this article are included in the article's Creative Commons license, unless indicated otherwise in a credit line to the material. If material is not included in the article's Creative Commons license and your intended use is not permitted by statutory regulation or exceeds the permitted use, you will need to obtain permission directly from the copyright holder. To view a copy of this license, visit <http://creativecommons.org/licenses/by/4.0/>.

several exons were also preferentially skipped by slowing down the RNAPII⁸. Such effect could rely on preferential recruitment of repressive splicing factors by the slow polymerase in the proximity of the regulated exon, as demonstrated for the *CFTR* gene⁹. Nevertheless, when and how such specific coordination is achieved under physiological situations remains largely unknown.

Testis is the organ displaying the highest abundance of splice variants¹⁰. In particular, meiotic spermatocytes display exceptional transcriptional and splicing diversity^{10–12}. AS flexibility is exploited by meiotic cells to produce protein variants uniquely required for the peculiar processes involved in germ cell differentiation^{13,14}, but also to dictate the timing of their expression¹². An interesting example in this sense is offered by the *Spo11* gene, encoding the essential endonuclease that establishes DNA double strand breaks (DSBs) and initiates homologous recombination in meiosis^{15,16}. The *Spo11* gene encodes for two main protein isoforms (SPO11 α and β) which differ for exon 2 skipping (α) or inclusion (β). Early meiotic spermatocytes synthesize primarily SPO11 β , whereas SPO11 α becomes predominant in late meiosis¹⁷. Notably, the timing of *Spo11* AS parallels that of DSB formation during meiosis, with a first wave in leptotene/zygotene spermatocytes that affects autosomal chromosomes and a delayed one that preferentially marks the sex chromosomes in late pachytene. Transgenic mice expressing only SPO11 β were fully competent in establishing the first DSB wave, but late foci in sex chromosomes, which appear in concomitance with SPO11 α splicing, were suppressed, leading to inefficient X–Y pairing and recombination¹⁸. Thus, the *Spo11* splice variants appear to operate on distinct subsets of meiotic DSBs that are both essential for gamete differentiation¹⁸. However, in spite of its physiological importance, the mechanism(s) underlying *Spo11* AS during meiosis are still unknown.

Herein, we describe a novel mechanism involved in the regulation of *Spo11* AS. We found that hnRNPH strongly induces SPO11 α splicing. Interestingly, hnRNPH was not upregulated in pachytene spermatocytes when the switch in splicing choice occurs. However, splicing regulation was paralleled by a decrease in the RNAPII elongation rate within the *Spo11* transcription, which promoted hnRNPH recruitment and exon 2 skipping. Mechanistically, hnRNPH competed for binding and splicing of the *Spo11* pre-mRNA with Sam68, a splicing factor whose ablation causes meiotic defects¹⁹. Thus, our work uncovers a fine-tuned combinatorial mechanism underlying the timely regulation of *Spo11* splicing during meiosis.

Results

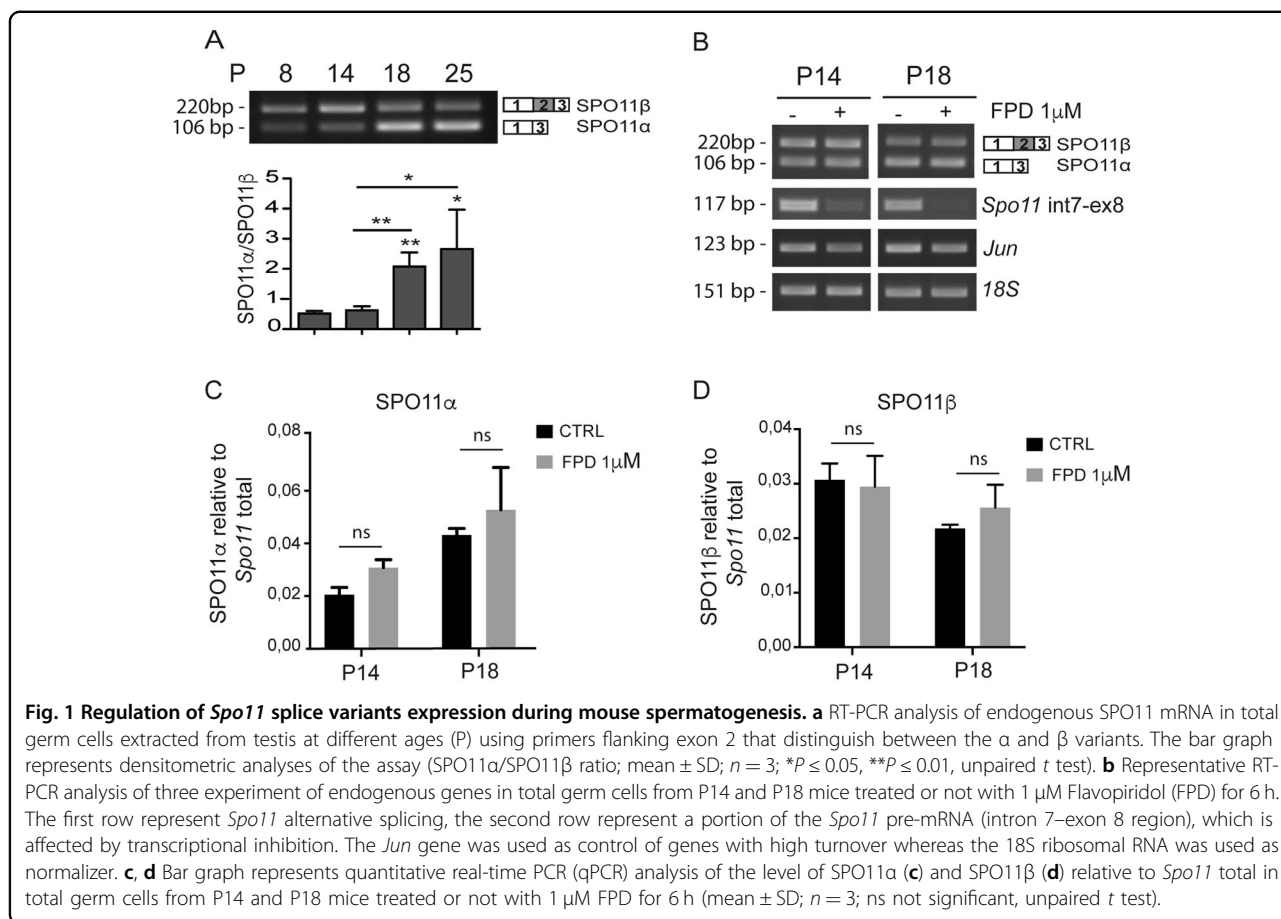
HnRNPH is a strong modulator of SPO11 α splicing

To determine the timing of *Spo11* splicing regulation, we isolated germ cells from CD1 mice during the first spermatogenic wave (8–25 postnatal day, P), when fronts

of germ cells almost synchronously enter into specific differentiation stages²⁰. As observed in another strain¹⁷, SPO11 β was the predominant variant expressed at P8 and P14 (Fig. 1a; Supplementary Fig. S1A), when testis is mostly populated by mitotic spermatogonia and early meiotic spermatocytes²⁰, respectively. By contrast, SPO11 α becomes the main variant at P18 and P25 (Fig. 1a; Supplementary Fig. S1A), when the most abundant cells are meiotic spermatocytes²⁰. Treatment with the RNAPII inhibitor flavopiridol (FPD) to block transcription¹² showed no significant changes in the stability of SPO11 α and SPO11 β mRNAs at these stages (Fig. 1b–d). These results suggest that a shift in *Spo11* splicing regulation occurs between P14 and P18.

We accurately staged male germ cells by monitoring assembly of the synaptonemal complex in chromosome spreads at P14 and P18²¹. Pachytene represents the longest stage of prophase I and early pachytene cells can be distinguished by the lack of expression of the testis-specific histone H1t, which becomes detectable in mid- and late-pachytene cells²⁰. Co-staining of chromosome spreads for the synaptonemal complex protein SCP3 and H1t did not reveal major changes in the population of meiotic spermatocytes between P14 and P18 (Supplementary Fig. S1B). Thus, changes in *Spo11* AS do not reflect a clear transition in meiosis.

Next, we searched for factors that could promote SPO11 α splicing. Analysis of binding sites within exon 2 and flanking intronic regions (100 base pair, bp) using the SpliceAid2 tool (http://193.206.120.249/splicing_tissue.html) identified several splicing factors potentially involved in *Spo11* AS in both human and mouse (Fig. 2a; Supplementary Fig. S2A). To test their effect on *Spo11* splicing, we constructed a minigene encompassing the genomic region from exon 1 to exon 3 (Fig. 2b). Splicing assays in human HEK293T cells, which do not express *SPO11*, indicated that the minigene yields both *Spo11* variants with a ratio comparable to that of P14 testis (Fig. 2c). Analysis of the predicted factors, as well as of other members of the SR and hnRNP families and of some tissue-specific splicing factors, revealed that hnRNPF and H were the strongest inducers of SPO11 α splicing (Fig. 2d, e; Supplementary Fig. S2B), whereas SRSF1, SRSF3, ETR-3, hnRNPA1/A2, RBM11, PTBP1/2 elicited a much milder effect. On the other hand, TRA2 α/β , Sam68, SLM2, and hnRNPK enhanced splicing of SPO11 β (Fig. 2d, e; Supplementary Fig. S2B). To test if differential expression of these splicing factors could account for the switch between P14 and P18, we performed Western blot analyses on germ cell extracts (Fig. 2f; Supplementary Fig. S2C). Remarkably, none of the tested factors displayed changes in expression compatible with their effect on *Spo11* AS, as most were unchanged between P14 and P18 (i.e.,

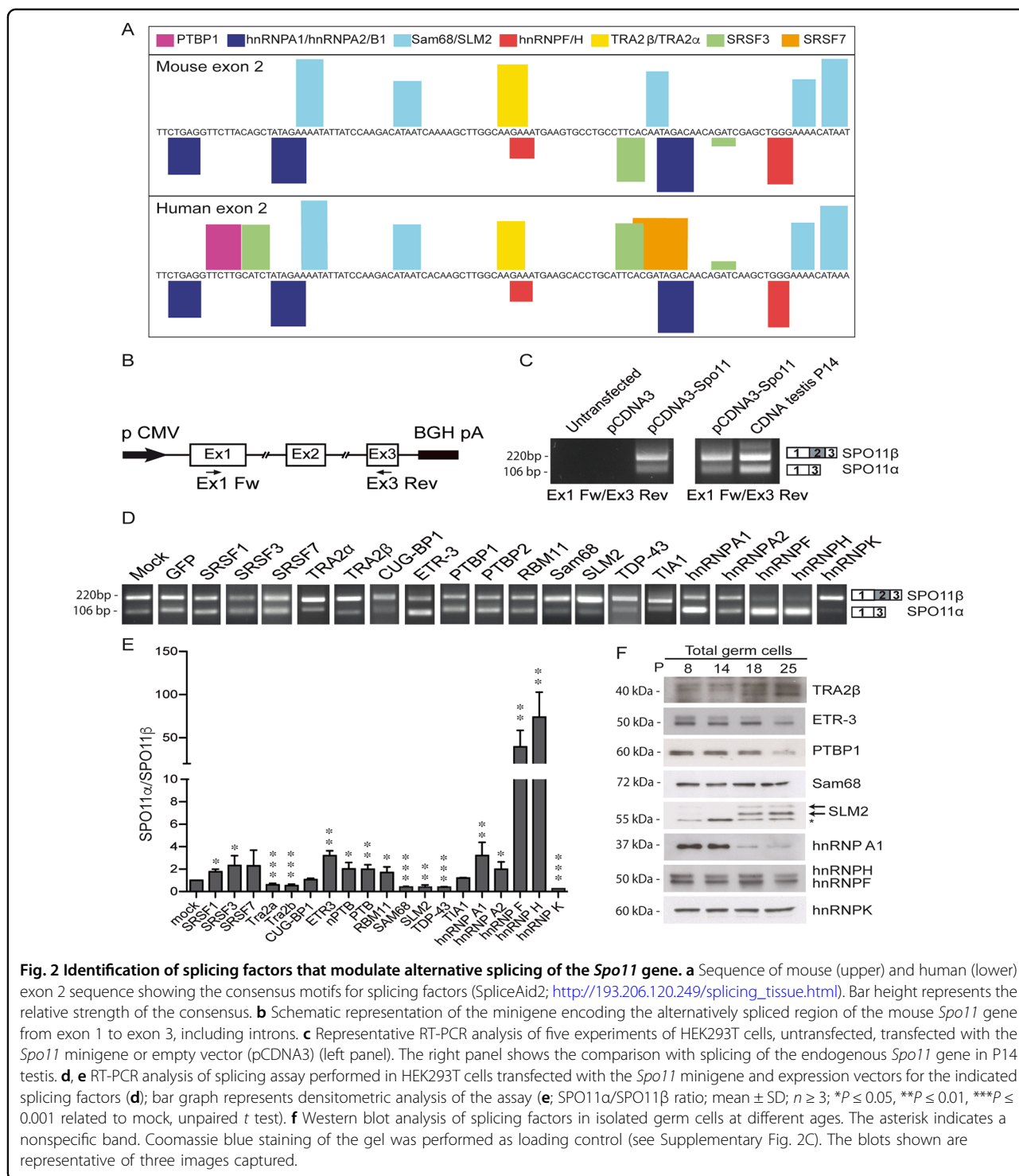


Sam68, hnRNPF/H, and PTBP1) or modulated in opposite direction with respect to their effect on *Spo11* splicing (hnRNPA1, SLM2, and ETR-3). Thus, the switch in SPO11 isoforms is unlikely due to differential expression of specific splicing factors during meiosis.

A reduced RNAPII elongation rate promotes splicing of SPO11 α

RNAPII processivity within the transcription unit can also influence AS regulation^{7–9,22}. Since RNAPII activity is modulated during male meiosis^{12,23}, we asked whether *Spo11* splicing is sensitive to changes in the RNAPII elongation rate. First, we measured RNAPII processivity as the ratio between expression of a distal vs. a proximal intron²⁴. To avoid issues related to intron stability in steady state transcript levels, we analyzed pulse-labeled pre-mRNAs synthesized *in vivo* in a limited time window (Fig. 3a). Mice were injected with 5-ethynyl uridine (EU) and its accumulation in nascent RNAs was monitored by immunofluorescence analysis. We found that a 2-h time frame was sufficient to yield efficient labeling of spermatocytes with EU *in vivo* (Supplementary Fig. 3A). Quantitative real-time polymerase chain reaction (qRT-PCR) analysis of EU-labeled transcripts showed that the

RNAPII elongation rate within *Spo11* is strongly reduced in P18 germ cells (Fig. 3b), concomitantly with exon 2 skipping and expression of SPO11 α (Fig. 1a). Moreover, analysis of other proximal regions (introns 2 and 3) in *Spo11* revealed that while all introns were efficiently represented in nascent transcripts at P14 (Fig. 3c), intron expression declined with distance from the transcriptional start site in P18 spermatocytes (Fig. 3d). These results suggest that the distal portion of the *Spo11* pre-mRNA accumulates at a slower rate at P18, in line with a reduced elongation rate of the polymerase. Such reduction was selective for the *Spo11* gene, as RNAPII processivity was unchanged within another meiotic gene (*Sycp1*) (Fig. 3b). Accordingly, by comparing P14 and P18 cell extracts we did not observe a general reduction in phosphorylation of RNAPII on Ser-2 (Supplementary Fig. 3B), which correlates with fast elongation rate²⁵. However, chromatin immunoprecipitation (ChIP) experiments highlighted a specific reduction of RNAPII phosphorylation in the exon 2 region of *Spo11* in P18 testis (Fig. 3e), which likely corresponds to slower rate and pausing of the polymerase, as we observed increased occupancy of total RNAPII near exon 2 (Fig. 3f) and a decline in nascent transcript accumulation downstream of it (Fig. 3d).



To test whether a slow RNAPII influences *Spo11* AS, we treated HEK293T cells with 5,6-dichloro-1-β-D-ribofuransylbenzimidazole (DRB) to reduce Ser-2 phosphorylation (Fig. 4a) and the RNAPII elongation rate⁸. DRB treatment strongly promoted splicing of SPO11α from the minigene (Fig. 4a). To confirm that a slow polymerase is

sufficient to induce this splicing switch, we engineered LNCaP cells to express an α-amanitin-resistant wild-type RPB1, encoding the large subunit of RNAPII, or the RPB1-R749H mutant, which reduces the elongation rate independently of phosphorylation²⁶. The basal splicing and the response to DRB of LNCaP cells transfected with

the *Spo11* minigene was similar to what observed in HEK293T cells (Supplementary Fig. 3C, D). Moreover, expression of RPB1-R749H mimicked the effect of DRB

and promoted SPO11 α splicing (Fig. 4b). These results suggest that changes in the RNAPII elongation rate within the *Spo11* locus modulate AS of exon 2 during meiosis.

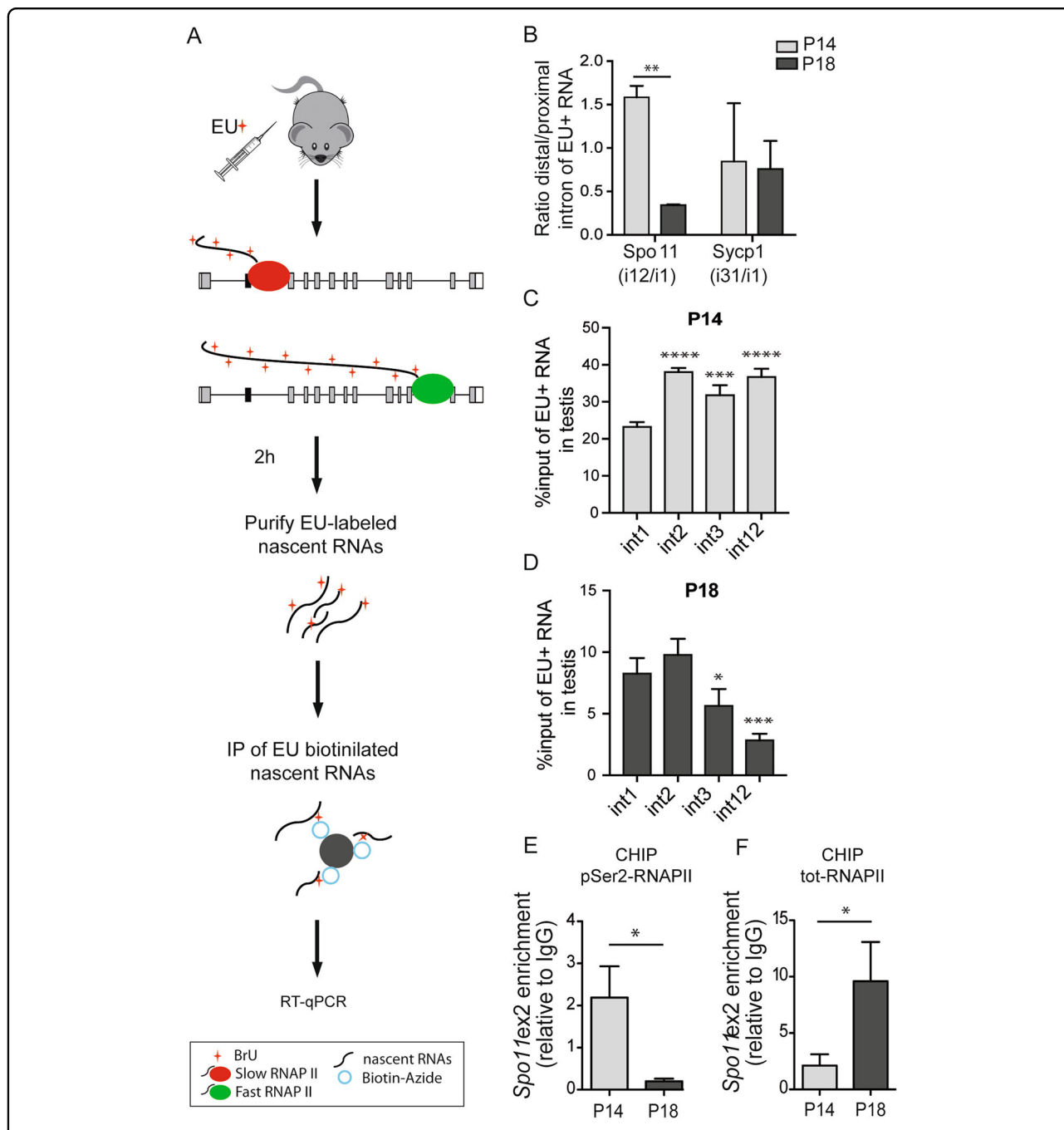


Fig. 3 The RNAPII elongation rate within the *Spo11* gene is modulated in meiosis. **a** Workflow used for detection of EU-labeled nascent RNAs. P14 and P18 mice were treated by intraperitoneal injection of EU (300 μ g/g). EU-labeled newly synthesized RNAs were collected from testes 2 h after injection, biotinylated and captured by streptavidin magnetic beads for analysis. **b** qPCR analysis of nascent *Spo11* and *Sycp1* transcripts from P14 and P18 mouse testis. The graph represents the ratio between distal and proximal intron of EU-labeled RNA. (mean \pm SD; $n = 3$; $**P \leq 0.01$, unpaired t test). **c, d** qPCR analysis of different regions of the nascent *Spo11* pre-mRNA corresponding in P14 (**c**) and P18 (**d**) mouse testis (mean \pm SD; $n = 3$; $*P \leq 0.05$, $**P \leq 0.01$, $***P \leq 0.001$ and $****P \leq 0.0001$ related to int1, one-way ANOVA, Bonferroni's multiple comparisons test). **e, f** ChIP assays of serine 2-phosphorylated (**d**) or total (**e**) RNAPII in the exon 2 region of *Spo11* in testicular germ cells at P14 and P18. The bar graph shows qPCR signals expressed as enrichment relative to IgG (mean \pm SD, $n = 3$; $*P \leq 0.05$, unpaired t test).

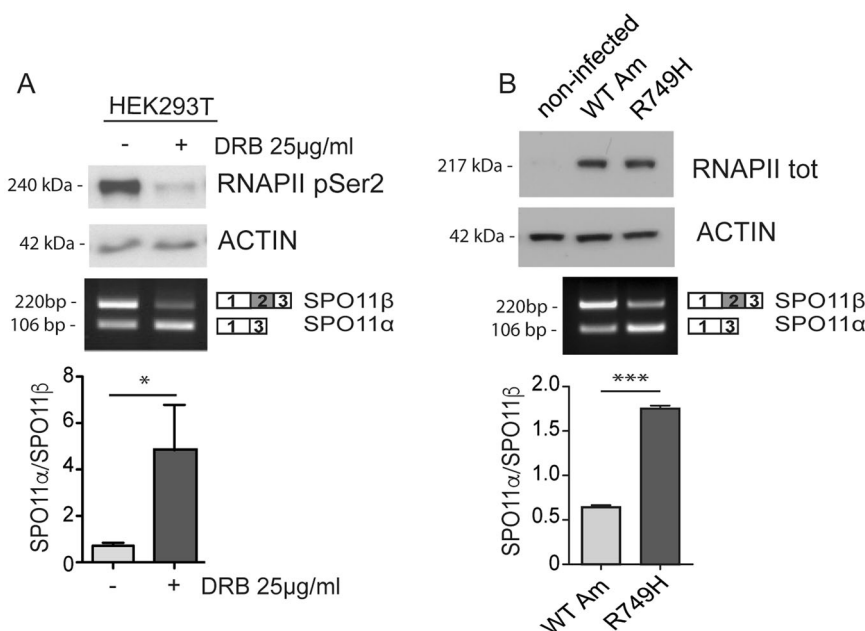


Fig. 4 Reduction of the RNAPII elongation rate promotes SPO11 α splicing. **a** Western blot and RT-PCR analyses of a representative splicing assay performed in HEK293T cells transfected with the *Spo11* minigene and treated with DRB (25 μ g/ml) for 16 h. The bar graph represents densitometric analyses of the SPO11 α /SPO11 β ratio (mean \pm SD, $n = 3$; $*P \leq 0.05$, unpaired t test). The Western blot analysis shows the levels of serine 2-phosphorylated RNAPII in the HEK293T cells used for the assay. **b** Western blot and RT-PCR analysis of a representative *Spo11* minigene splicing assay performed in LNCaP cells stably infected with the lentiviral vector pLV-Rbp1-WT-Am^r or pLV-Rbp1-R749H-Am^r and treated with 2 μ g/ml of α -amanitin for 48 h, when endogenous RNAPII was inactive (mean \pm SD, $n = 3$; $***P \leq 0.001$, unpaired t test). The Western blot analysis shows the similar levels of expression of recombinant wild-type and mutant RNAPII in the infected LNCaP cells used for the experiment. The noninfected cells show absence of endogenous RNAPII after treatment with α -amanitin for 48 h. The blots shown are representative of three images captured (**a**, **b**).

A slow RNAPII favors recruitment of hnRNPH and skipping of exon 2 in *Spo11* pre-mRNA

Phosphorylation of the carboxyl-terminal domain of RNAPII modulates its interaction with splicing factors during pre-mRNA processing²⁷. As hnRNPH strongly induced SPO11 α splicing, we focused on this factor. First, we evaluated whether hnRNPH interacts with RNAPII. Co-immunoprecipitation experiments revealed a weak interaction of hnRNPH with the polymerase under basal conditions (Fig. 5a). However, DRB-mediated inhibition of RNAPII Ser-2 phosphorylation promoted its association with hnRNPH (Fig. 5a), without affecting hnRNPH expression (Supplementary Fig. 4A, B). UV cross-link immunoprecipitation (CLIP) experiments demonstrated that direct binding of hnRNPH to the *Spo11* pre-mRNA was also significantly enhanced by DRB treatment (Fig. 5b), suggesting that hnRNPH association with RNAPII promotes its recruitment to the target pre-mRNA. Likewise, CLIP experiments documented that hnRNPH binding to *Spo11* pre-mRNA is increased in vivo in P18 testes (Fig. 5c), concomitantly with the reduction of RNAPII processivity (Fig. 3b) and SPO11 α splicing (Fig. 1a).

Next, we asked if expression of hnRNPH is required for the effect of DRB on *Spo11* minigene splicing. Knockdown

of hnRNPH, and of its close homolog hnRNPF, reduced SPO11 α splicing under basal conditions. Moreover, hnRNPF/H silencing almost completely abrogated the effect of DRB on the promotion of this splice variant (Fig. 5d), indicating that hnRNPH is involved in coupling RNAPII dynamics with *Spo11* splicing regulation.

A slow RNAPII was shown to promote ETR-3 recruitment and exon skipping in the *CFTR* gene⁹. Since ETR-3 binding sites are present in the *Spo11* alternatively spliced region (Fig. 2a, Supplementary Fig. 2A) and ETR-3 weakly promotes SPO11 α splicing (Fig. 2d, e), we asked whether it also acted in coupling RNAPII with *Spo11* AS. However, silencing of ETR-3 did not significantly modify the effect of DRB on exon 2 splicing and ETR-3 was bound to *Spo11* transcript in vivo only at P14 (Supplementary Fig. S4C, D). These experiments indicate a specific role for hnRNPH in the regulation of *Spo11* AS. Moreover, they suggest a combinatorial control of this event elicited by changes in RNAPII dynamics and the specific exon environment that selectively favor hnRNPH recruitment.

hnRNPH competes with Sam68 for the regulation of *Spo11* AS

HnRNPs often repress splicing by competing with recruitment of other factors or the spliceosome^{1,4}. To test

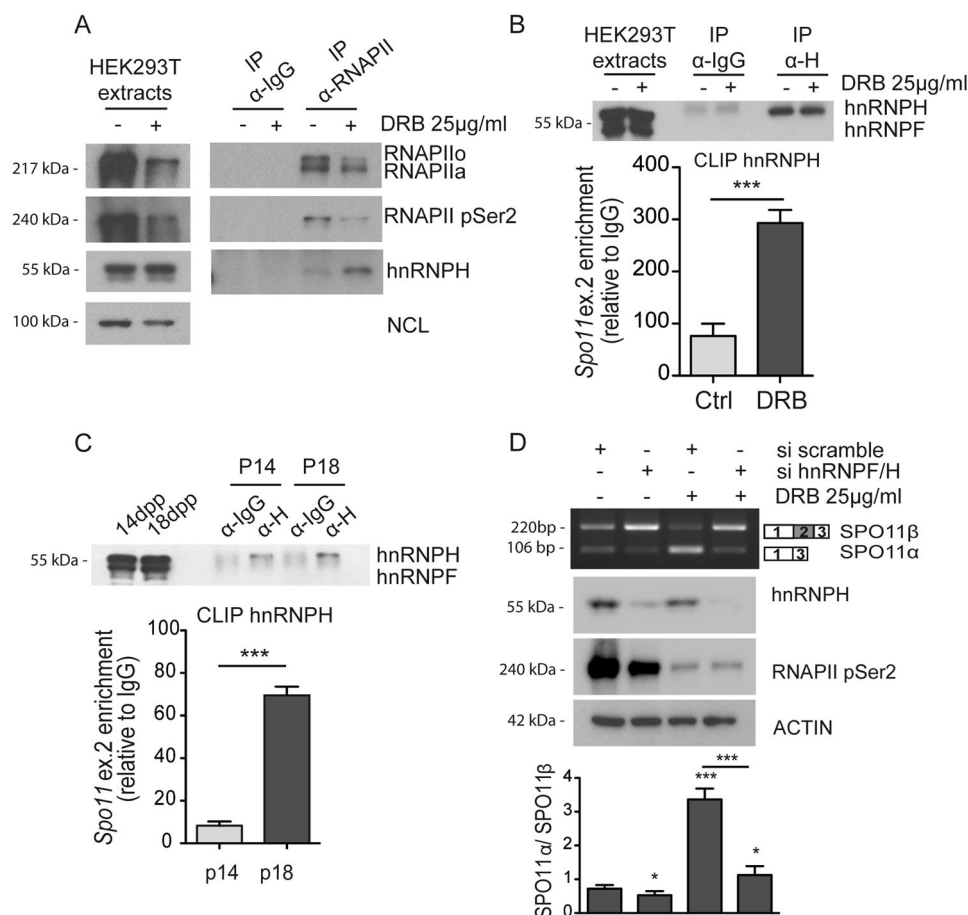
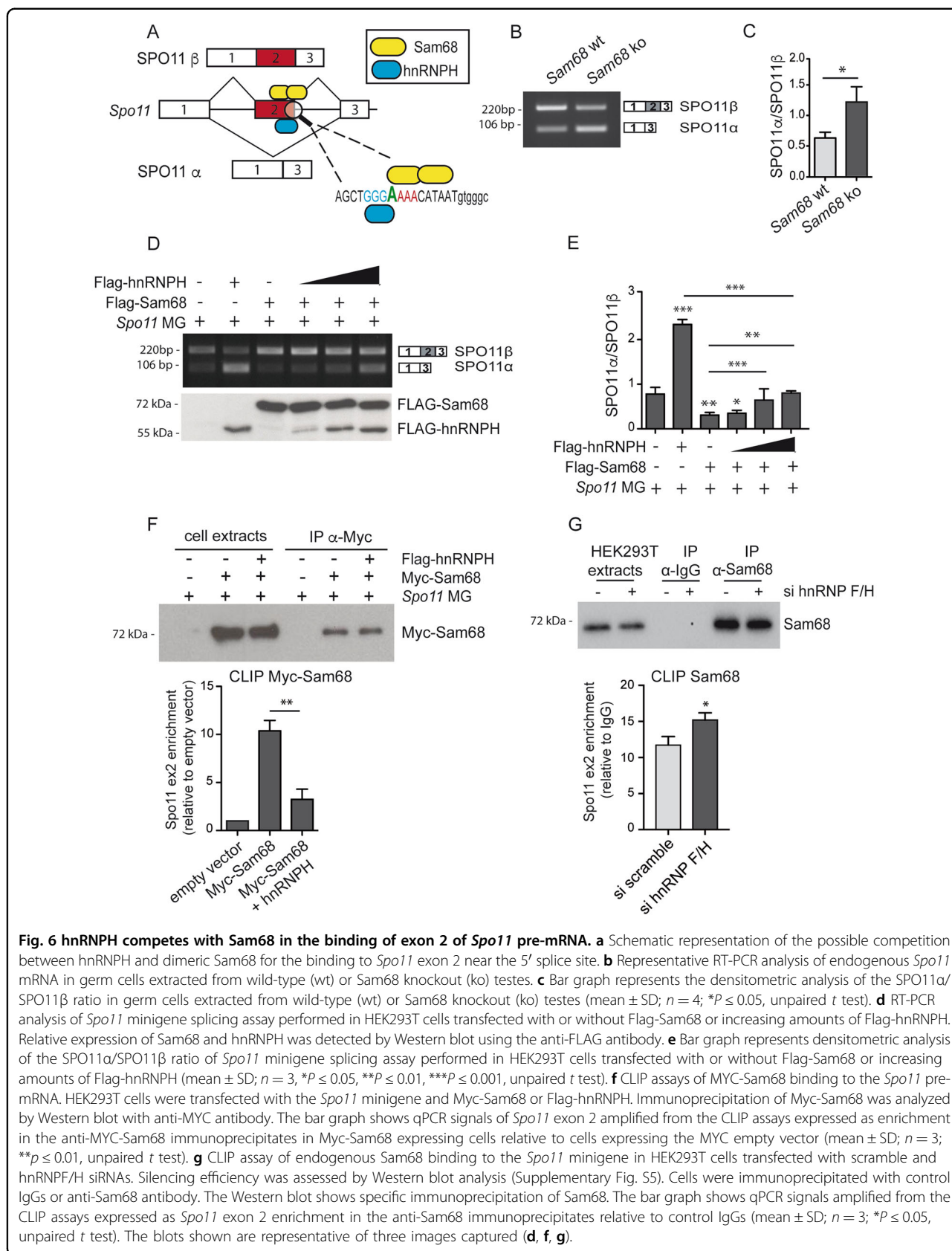


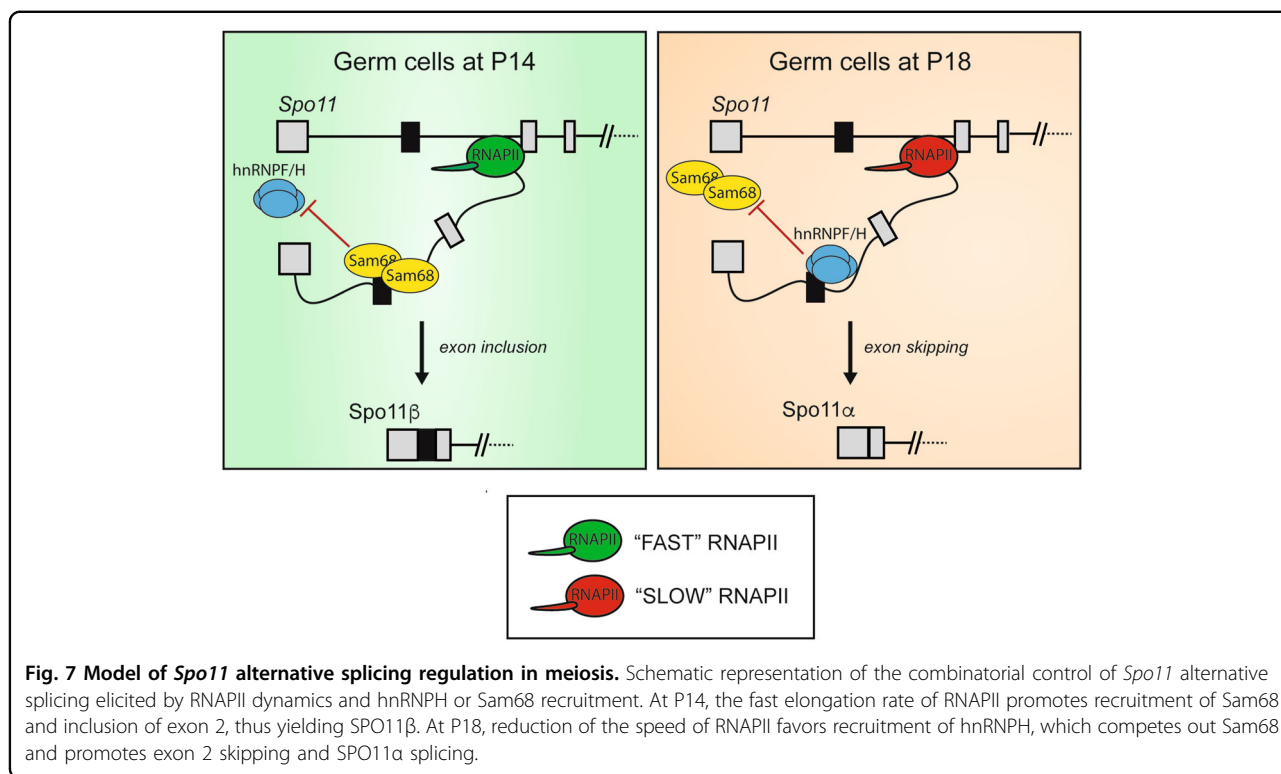
Fig. 5 A slow RNAPII favors recruitment of hnRNPF/H in the *Spo11* pre-mRNA. **a** Co-immunoprecipitation analysis performed in HEK293T cells treated or not with DRB (25 µg/ml). Nuclear extracts were immunoprecipitated with control IgGs or anti-RNAPII antibodies in the absence of RNase A and analyzed by Western blot for total and serine 2-phosphorylated RNAPII and hnRNPH. Nucleolin (NCL) was used as loading control for the nuclear extracts. **b** CLIP assay of hnRNPF/H binding to the *Spo11* minigene in transfected HEK293T cells treated or not with DRB (25 µg/ml). Cells were UV-cross-linked and immunoprecipitated with control IgGs or anti-hnRNPF/H antibody. The Western blot shows specific immunoprecipitation of hnRNPF/H. The bar graph shows qPCR signals amplified from the CLIP assays expressed as *Spo11* exon 2 enrichment in the anti-hnRNPF/H immunoprecipitates relative to control IgGs (mean ± SD; n = 3; ***P ≤ 0.001, unpaired t test). **c** CLIP assay of hnRNPF/H binding to the endogenous *Spo11* pre-mRNA. P14 and P18 mouse testes were UV-cross-linked and immunoprecipitated with control IgGs or anti-hnRNPF/H antibody. The Western blot shows specific immunoprecipitation of hnRNPF/H. The bar graph shows qPCR signals amplified from the CLIP assays expressed as *Spo11* exon 2 enrichment in the anti-hnRNPF/H immunoprecipitates relative to control IgGs (mean ± SD; n = 3; ***P ≤ 0.001, unpaired t test). **d** RT-PCR analysis of *Spo11* minigene splicing assays in HEK293T cells transfected with scramble and hnRNPF/H siRNAs. Silencing efficiency was assessed by Western blot analysis. Bar graph represents the densitometric analysis of the SPO11α/SPO11β ratio (mean ± SD; n = 3; *P ≤ 0.05, ***P ≤ 0.001, unpaired t test). The blots shown are representative of three images captured (**a-d**).

whether occupancy of regulatory sequences by hnRNPF/H promoted exon skipping by competing out positive regulators, we focused on Sam68 because its binding site is located in close proximity to that of hnRNPF/H (Fig. 6a). Sam68 promotes exon 2 inclusion (Fig. 2d, e) and it cooperates with the spliceosomal U1snRNP in exon recognition^{28,22}. Analysis of testes from juvenile *Sam68* knockout mice (P10) showed a significant reduction in *Spo11* exon 2 inclusion (Fig. 6b, c), suggesting the physiological relevance of Sam68-mediated regulation. To test whether hnRNPF/H competes with Sam68 for *Spo11* AS regulation, we performed splicing assays with a

concentration of Sam68 that induced almost complete splicing of the SPO11β variant and increasing amounts of hnRNPF/H. We observed a dose-dependent reversion of splicing with increasing hnRNPF/H levels (Fig. 6d, e). However, even at its highest dose, hnRNPF/H was unable to completely switch splicing toward the SPO11α variant in the presence of Sam68 overexpression.

To test whether hnRNPF/H competes with Sam68 for binding to exon 2, we performed CLIP assays in HEK293T cells transfected with the *Spo11* minigene. Sam68 was efficiently recruited to the *Spo11* pre-mRNA when expressed alone. However, its binding was strongly





reduced when hnRNPH was overexpressed (Fig. 6f). By contrast, hnRNPF/H knockdown caused a small but significant increase in the binding of Sam68 to the *Spo11* pre-mRNA (Fig. 6g). These findings suggest that binding of hnRNPF near specific regulatory regions hinders the recruitment of Sam68, thus promoting exon 2 skipping from the *Spo11* pre-mRNA.

Discussion

Male germ cells display the highest complexity in gene expression and AS regulation among mammalian tissues^{10,12}. This extensive utilization of the coding potential and plasticity of the genome may underlie the unique features required for germ cell differentiation²⁹. One such unique feature is the timely appearance in early meiosis of DSBs driven by SPO11^{15,16}, which allow recombination, pairing and proper segregation of homologous chromosomes³⁰. Notably, the main SPO11 splice variants, SPO11α and β, are differentially expressed in spermatocytes and both are necessary for proper meiosis¹⁸. Nevertheless, how temporal regulation of *Spo11* splicing is achieved is currently unknown. Herein, we have identified a combinatorial control that insures *Spo11* AS regulation at a specific time in meiosis, which relies on the concerted action of RNAPII and the splicing factor hnRNPF. A fast RNAPII elongation rate in early meiosis prevents binding of hnRNPF to the *Spo11* pre-mRNA, whereas the reduced

speed of RNAPII in late meiosis promotes hnRNPF recruitment and skipping of exon 2 (Fig. 7). These findings uncover a novel modality of developmental regulation of splicing that couples changes in RNAPII dynamics with specific recruitment of splicing factors during meiosis, thus guaranteeing accurate control of SPO11 isoform expression in the differentiating gametes.

HnRNPH, and its close homolog hnRNPF, are potent regulators of exon 2 skipping. Interestingly, in primary germ cells hnRNPH is differentially recruited in proximity of the *Spo11* exon 2 splice site at P14 and P18, even though its expression level remains unchanged. However, we found that recruitment of hnRNPF to *Spo11* exon 2 sequences is sensitive to RNAPII dynamics, whose regulation during meiosis has been documented^{12,31,32}. Several lines of evidence support this conclusion. First, interaction of hnRNPF and RNAPII is promoted by Ser-2 dephosphorylation; second, RNAPII phosphorylation in Ser-2 and RNAPII processivity within the *Spo11* locus are modulated during meiosis; third, decreased processivity correlates with recruitment of hnRNPF to exon 2 in the *Spo11* pre-mRNA; fourth, ectopic manipulation of RNAPII dynamics recapitulates regulation of SPO11α splicing in an hnRNPF-dependent fashion. These findings suggest that a fast RNAPII elongation rate prevents binding of hnRNPF/H to the *Spo11* pre-mRNA, allowing its recognition by positive regulators that promote SPO11β

splicing (Fig. 7). Reduced speed of RNAPII later in meiosis, instead, favors recruitment of hnRNPH, leading to displacement of positive regulators and splicing of SPO11 α . This competition-based mechanism is also supported by the observation that the strongest hnRNPH binding sites in exon 2 overlap with the consensus motif for Sam68, which promotes SPO11 β splicing. Thus, occupancy of the region flanking the 5' splice site by hnRNPH may prevent recruitment of positive regulators (i.e., Sam68) that are necessary for efficient exon 2 definition. Mechanistically, since Sam68 cooperates with U1snRNP to promote exon recognition in male germ cells³¹, binding of hnRNPH to the exon 2–intron 2 region may disrupt this interaction at P18 and cause the switch in SPO11 isoforms. Thus, our work suggests that combinatorial control of RNAPII dynamics and recruitment of specific splicing factors may dictate temporal regulation of a splicing pattern during meiosis.

The physiological relevance of most annotated splice variants remains largely unknown. In the case of SPO11, expression of SPO11 β alone was not sufficient to fully compensate for the ablation of the gene¹⁸. SPO11 β -only mice were defective in pairing of the X–Y chromosomes in late meiosis, suggesting that SPO11 α plays a nonredundant role and physiologically compensates for this defect¹⁸. This observation also indicates that lack of proper SPO11 α splicing during meiosis exposes to higher risk of sex chromosomes aneuploidy, a pathological condition that gives rise to human diseases like the Klinefelter syndrome³³. Thus, while changes in *Spo11* expression levels can be tolerated to some extent by homeostatic mechanisms that control crossover formation³⁴, lack of expression of a splice variant of the gene yields non rescuable defects. In this scenario, our findings provide mechanistic insights into the temporal control of *Spo11* splicing during meiosis and point to hnRNPH and Sam68 as key regulators of this process. Notably, *Sam68* knockout spermatocytes undergo apoptosis in late meiosis¹⁹. Thus, our findings also suggest that dysregulation of SPO11 α expression may cause defective homologous recombination in vivo, resulting in increased meiotic cell death.

Materials and methods

Germ cells isolation and culture

Germ cells were obtained from testes of Swiss CD-1 mice as reported²³. Briefly, after testis digestion with collagenase and trypsin, the cell suspension was plated for 4 h in minimum essential medium (MEM), supplemented with 1 mM DL-lactic acid, 2 mM sodium pyruvate, 10% fetal calf serum, to promote adhesion of somatic cells. Germ cells that remain in suspension were then collected. For transcription inhibition, following two washes in MEM, germ cells were released for 6 h in fresh medium added or not with 1 μ M FPD (Sigma-Aldrich) and then harvested for analysis.

Spo11 minigene construct and PCR analyses

The *Spo11* minigene was amplified from genomic DNA of P14 mouse testis using primers reported in the Supplementary Table, cloned into pCDNA3.1(–) vector, and validated by sequencing.

For PCR analyses, RNA from samples was extracted using TRIzol reagent (Invitrogen), digested with RNase-free DNase (Roche), retrotranscribed (1 μ g) using M-MLV reverse transcriptase (Promega) and used for PCR reactions (GoTaq, Promega). RT-qPCR analyses were performed using LightCycler 480 SYBR Green I Master with the LightCycler 480 System (Roche). Control reactions omitted M-MLV reverse transcriptase. Primers are listed in the Supplementary Table 1.

Cell culture, transfections, and treatment

HEK293T cells were grown in Dulbecco's modified Eagle's medium (Sigma Aldrich), supplemented with 10% fetal bovine serum (FBS) (Gibco), gentamicin sulfate (50 g/ml) (Aurogene), 1% nonessential aminoacids (Euroclone), penicillin (50 U/ml)/streptomycin (50 g/ml) (Corning). LNCaP cells were grown in RPMI 1640 medium (LONZA), supplemented with 10% FBS (Gibco), penicillin (50 U/ml)/streptomycin (50 g/ml) (Corning), gentamicin sulfate (50 g/ml) (Aurogene), 1% nonessential aminoacids (Euroclone), 10 mM Hepes (Euroclone), and 1 mM sodium pyruvate (Aurogene). Transfections were performed using Lipofectamine 2000 (Invitrogen) and 2 μ g of pCDNA3.1-*Spo11* minigene with or without expression vectors for the indicated proteins; 6 h after transfection, cells were treated or not with 25 μ g/ml DRB for 16 h before harvest. For RNA interference, cells were transfected with appropriate siRNAs (Sigma-Aldrich) using Lipofectamine RNAiMAX (Invitrogen) and harvested 48 h later for analyses.

Pull-down assay of nascent RNAs

Testis of P14 and P18 mice were collected after 2 h of intraperitoneal injection of EU (Life Technologies) or PBS as control, as described¹². Samples were collected in Trizol and RNA was isolated, biotinylated and captured using the Click-IT Nascent RNA Capture kit (Life Technologies). Captured nascent RNAs were retrotranscribed using the SuperScript VILO cDNA Synthesis Kit (Life Technologies) followed by qPCR analysis.

Cross-link immunoprecipitation (CLIP) experiments

CLIP experiments were performed as described³⁵. Briefly, HEK293T cells and testicular cells were irradiated on ice (400 mJ/cm²) in PBS, scraped off and centrifuged for 5 min at 300g at 4 °C. After sample processing, extracts (0.5–1 mg) were immunoprecipitated using anti-hnRNPH (provided by Prof. B. Chabot, Université de Sherbrooke, Canada), anti-MYC (Santa Cruz Biotechnology) or rabbit IgG (control) in

the presence of protein G magnetic (Life Technologies). After stringent washes and Proteinase K treatment (1 h at 55 °C), RNA was isolated by standard procedures, retro-transcribed with random primers, and M-MLV reverse transcriptase (Promega) and used for qPCR. RNA associated with hnRNPH is represented as fold enrichment relative to IgG samples, RNA associated with MYC is represented as fold enrichment relative to empty vector.

ChIP assay

ChIP was performed as described³⁶ using P14 and P18 testes crosslinked in 1% (vol/vol) formaldehyde for 10 min at room temperature and quenched with 125 mM glycine for 5 min.

Statistical analysis

Statistical tests were performed by the Student *t* test or One-Way ANOVA using GraphPad Prism6; $P \leq 0.05$ was considered significant. No analyses were used to pre-determine sample size. The experiments were not randomized and investigators were not blinded to allocation during experiments and outcome assessment.

Acknowledgements

We wish to thank Dr. M. Barchi for fruitful discussion throughout this work and Drs. M.A. Handel, B. Chabot, D. Elliott for providing antibodies used in this study, Dr. E. Buratti for providing the TDP-43 vector. This work was supported by Telethon (GGP12189), by Associazione Italiana Ricerca sul Cancro (AIRC) and by the UCSC grant Linea D1. C.N. was supported in part by a scholarship from Fondazione Umberto Veronesi. Supplementary information is available at Cell Death & Disease's website.

Author details

¹Department of Neuroscience, Section of Human Anatomy, Catholic University of the Sacred Heart, 00168 Rome, Italy. ²Laboratory of Neuroembryology, IRCCS Fondazione Santa Lucia, 00143 Rome, Italy. ³Department of Biomedicine and Prevention, University of Rome Tor Vergata, 00133 Rome, Italy

Conflict of interest

The authors declare that they have no conflict of interest.

Publisher's note

Springer Nature remains neutral with regard to jurisdictional claims in published maps and institutional affiliations.

Supplementary Information accompanies this paper at (<https://doi.org/10.1038/s41419-020-2443-y>).

Received: 4 January 2020 Revised: 27 February 2020 Accepted: 28 February 2020

Published online: 17 April 2020

References

- Fu, X. & Ares, M. J. Context-dependent control of alternative splicing by RNA binding proteins. *Nat. Rev. Genet.* **15**, 689–701 (2014).
- Paronetto, M. P., Passacantilli, I. & Sette, C. Alternative splicing and cell survival: from tissue homeostasis to disease. *Cell Death Differ.* **23**, 1919–1929 (2016).
- Will, C. L. & Lührmann, R. Spliceosome structure and function. *Cold Spring Harb. Perspect. Biol.* **3**, 1–2 (2011).
- Matera, A. G. & Wang, Z. A day in the life of the spliceosome. *Nat. Rev. Mol. Cell Biol.* **15**, 108–121 (2014).
- Luco, R. F., Allo, M., Schor, I. E., Kornblihtt, A. R. & Misteli, T. Epigenetics in alternative pre-mRNA splicing. *Cell* **144**, 16–26 (2011).
- Naftelberg, S., Schor, I. E., Ast, G. & Kornblihtt, A. R. Regulation of alternative splicing through coupling with transcription and chromatin structure. *Annu. Rev. Biochem.* **84**, 165–198 (2015).
- De La Mata, M. et al. A slow RNA polymerase II affects alternative splicing in vivo. *Mol. Cell* **12**, 525–532 (2003).
- Ip, J., Schmidt, D. & Pan, Q. Global impact of RNA polymerase II elongation inhibition on alternative splicing regulation. *Genome Res.* **21**, 390–401 (2011).
- Dujardin, G. et al. How slow RNA polymerase II elongation favors alternative exon skipping. *Mol. Cell* **54**, 683–690 (2014).
- Soumillon, M. et al. Cellular source and mechanisms of high transcriptome complexity in the mammalian testis. *Cell Rep.* **3**, 2179–2190 (2013).
- Schmid, R. et al. The splicing landscape is globally reprogrammed during male meiosis. *Nucleic Acids Res.* **41**, 10170–10184 (2013).
- Naro, C. et al. An orchestrated intron retention program in meiosis controls timely usage of transcripts during germ cell differentiation. *Dev. Cell* **41**, 82–93.e4 (2017).
- Elliott, D. J. & Grellscheid, S. N. Alternative RNA splicing regulation in the testis. *Reproduction* **132**, 811–819 (2006).
- Paronetto, M. P. & Sette, C. Role of RNA-binding proteins in mammalian spermatogenesis. *Int. J. Androl.* **33**, 2–12 (2010).
- Baudat, F., Manova, K., Yuen, J. P., Jasin, M. & Keeney, S. Chromosome synapsis defects and sexually dimorphic meiotic progression in mice lacking Spo11. *Mol. Cell* **6**, 989–998 (2000).
- Romanienko, P. J. & Camerini-Otero, R. D. The mouse Spo11 gene is required for meiotic chromosome synapsis. *Mol. Cell* **6**, 975–987 (2000).
- Bellani, M. A., Boateng, K. A., McLeod, D. & Camerini-Otero, R. D. The expression profile of the major mouse SPO11 isoforms indicates that SPO11 introduces double strand breaks and suggests that SPO11 has an additional role in prophase in both spermatocytes and oocytes. *Mol. Cell Biol.* **30**, 4391–4403 (2010).
- Kauppi, L. et al. Distinct properties of the XY pseudoautosomal region crucial for male meiosis. *Science* **331**, 916–920 (2011).
- Paronetto, M. P. et al. Sam68 regulates translation of target mRNAs in male germ cells, necessary for mouse spermatogenesis. *J. Cell Biol.* **185**, 235–249 (2009).
- Bellve, A. R. et al. Spermatogenic cells of the prepubertal mouse. Isolation and morphological characterization. *J. Cell Biol.* **74**, 68–85 (1977).
- Moens, P. B., Heyting, C., Dietrich, A. J., vanRaamsdonk, W. & Chen, Q. Synaptonemal complex antigen localization and conservation. *J. Cell Biol.* **105**, 93–103 (1987).
- Subramania, S. et al. SAM68 interaction with U1A modulates U1 snRNP recruitment and regulates mTOR pre-mRNA splicing. *Nucleic Acids Res.* **47**, 4181–4197 (2019).
- Paronetto, M. P. et al. Sam68 marks the transcriptionally active stages of spermatogenesis and modulates alternative splicing in male germ cells. *Nucleic Acids Res.* **39**, 4961–4974 (2011).
- Batsché, E., Yaniv, M. & Muchardt, C. The human SWI/SNF subunit Brm is a regulator of alternative splicing. *Nat. Struct. Mol. Biol.* **13**, 22–29 (2006).
- Phatnani, H. P. & Greenleaf, A. L. Phosphorylation and functions of the RNA polymerase II CTD. *Genes Dev.* **20**, 2922–2936 (2006).
- Fong, N. et al. Pre-mRNA splicing is facilitated by an optimal RNA polymerase II elongation rate. *Genes Dev.* **28**, 2663–2676 (2014).
- Hsin, J. & Manley, J. L. The RNA polymerase II CTD coordinates transcription and RNA processing. *Genes Dev.* **26**, 2119–2137 (2012).
- Naro, C. et al. Functional Interaction between U1snRNP and Sam68 insures proper 3' end pre-mRNA processing during germ cell differentiation. *Cell Rep.* **26**, 2929–2941.e5 (2019).
- Griswold, M. D. Spermatogenesis: the commitment to meiosis. *Physiol. Rev.* **96**, 1–17 (2016).
- Keeney, S., Lange, J. & Mohibullah, N. Self-organization of meiotic recombination initiation: general principles and molecular pathways. *Annu. Rev. Genet.* **48**, 187–214 (2014).
- Turner, J. M. A. et al. Silencing of unsynapsed meiotic chromosomes in the mouse. *Nat. Genet.* **37**, 41–47 (2005).
- Bielli, P., Busà, R., Paronetto, M. P. & Sette, C. The RNA-binding protein Sam68 is a multifunctional player in human cancer. *Endocr. Relat. Cancer* **18**, R91–R102 (2011).

33. Thomas, N. S. & Hassold, T. J. Aberrant recombination and the origin of Klinefelter syndrome. *Hum. Reprod. Update* **9**, 309–317 (2003).
34. Cole, F. et al. Homeostatic control of recombination is implemented progressively in mouse meiosis. *Nat. Cell Biol.* **14**, 424–430 (2012).
35. Bielli, P. & Sette, C. Analysis of in vivo interaction between RNA binding proteins and their RNA targets by UV cross-linking and immunoprecipitation (CLIP) method. *Bio-Protocol*. <https://doi.org/10.21769/bioprotoc.2274> (2017).
36. Cappellari, M. et al. The transcriptional co-activator SND1 is a novel regulator of alternative splicing in prostate cancer cells. *Oncogene* **33**, 3794–3802 (2014).